

RESEARCH ARTICLE | NOVEMBER 23 2021

Formation of density corrugations due to zonal flow in wave-kinetic framework

M. Sasaki   ; K. Itoh; B. F. McMillan  ; T. Kobayashi  ; H. Arakawa  ; J. Chowdhury 



Phys. Plasmas 28, 112304 (2021)

<https://doi.org/10.1063/5.0055777>



Physics of Plasmas
Features in Plasma Physics Webinars

Register Today!



Formation of density corrugations due to zonal flow in wave-kinetic framework

Cite as: Phys. Plasmas **28**, 112304 (2021); doi: [10.1063/5.0055777](https://doi.org/10.1063/5.0055777)

Submitted: 3 May 2021 · Accepted: 28 October 2021 ·

Published Online: 23 November 2021



View Online



Export Citation



CrossMark

M. Sasaki,^{1,a)}  K. Itoh,^{2,3} B. F. McMillan,⁴  T. Kobayashi,⁵  H. Arakawa,⁶  and J. Chowdhury^{7,b)}

AFFILIATIONS

¹College of Industrial Technology, Nihon University, Narashino 275-8575, Japan

²Frontier Research Institute, Chubu University, Kasugai, Aichi 487-8501, Japan

³Research Center for Plasma Turbulence, Kyushu University, Kasuga 816-8580, Japan

⁴Centre for Fusion, Space and Astrophysics, Department of Physics, Warwick University, Coventry CV4 7AL, United Kingdom

⁵National Institute for Fusion Science, National Institutes of Natural Sciences, Toki 509-5292, Japan

⁶Institute of Science and Engineering, Academic Assembly, Shimane University, Matsue 690-8504, Japan

⁷Department of Physics, Sikkim University, Gangtok, Sikkim 737102, India

a) Author to whom correspondence should be addressed: sasaki.makoto@nihon-u.ac.jp

b) Current address: Institute for Plasma Research, Bhat, Gandhinagar, 382428, India

ABSTRACT

The formation of density corrugation due to zonal flow, so-called zonal staircase, is investigated theoretically, based on the wave-kinetic framework. The wave-kinetic simulation is performed, considering the profile corrugation and the turbulence trapping mechanism, where the profile corrugation changes the growth rate and the dispersion relation of turbulence. The zonal density is generated by the modulation of particle transport. We obtain the analytical expression for the zonal density, which determines the staircase height. It is found that the amplitude normalized by the ambient density can be comparable to the zonal flow normalized by the diamagnetic drift velocity. The key effect that determines the turbulence profile is found to be the phenomenon of turbulence trapping by zonal flow, while the profile corrugation due to zonal density has weaker effects. Thus, turbulence is localized where the flow curvature is negative, which leads to a flattening of the density profile through the enhancement of particle transport. This fact clearly shows that the effect of turbulence trapping dominates the density gradient dependence of the local linear instability.

Published under an exclusive license by AIP Publishing. <https://doi.org/10.1063/5.0055777>

I. INTRODUCTION

The formation of staircase-like profile corrugations is universal in fluid phenomena such as fusion plasmas, oceans, and atmosphere.^{1–3} In magnetically confined plasmas, the staircases have been observed in the fluid turbulence model⁴ and gyro-kinetic simulations^{3,5–8} for various turbulence modes such as ion temperature gradient mode and trapped electron mode. Staircases in many cases have been found to accompany the formation of perpendicular flows ($E \times B$ and zonal flow). In recent experiments, highly accurate profile measurement methods have been developed, and staircases with the coexistence of flows have been reported.^{9–12} A theoretical understanding of staircase formation due to the interaction of turbulence and flows is of great importance.

Staircase formation is a result of profile corrugations; thus, the interaction between turbulence and zonal flows as well as the profile

relaxation processes should be considered simultaneously. In the process of the turbulence–zonal flow interactions, turbulence trapping by zonal flow has been found to play a crucial role in determining the spatial distribution of the phenomenon of turbulence.^{13–16} Here, turbulence trapping appears as a dynamic effect in phase space, where the phase space consists of the real and wavenumber spaces, and thus the wave-kinetic theory is suitable to consider this process. Actually, asymmetric turbulence intensity with respect to the sign of flow curvature, which is characteristic of turbulence trapping, has been observed in several turbulence simulations.^{5,17} On the contrary, the theoretical model for the staircases based on the jam of the turbulence avalanche¹⁸ has been reported¹⁹ without considering the interaction with the flow, explicitly. The zonal flow effect has been included in Ref. 20 for a staircase analysis based on the mixing length theory, which is not enough to consider the phase space dynamics of turbulence.

In this study, the zonal-staircase formation is investigated by considering the phase space dynamics (turbulence trapping mechanism), based on a wave-kinetic framework. The self-consistent simulation is performed, where the profile relaxation and turbulence–zonal flow interaction are simultaneously included. It is shown that turbulence trapping is significant for the spatial structures of zonal staircases. An analytical expression for the zonal-staircase height is also obtained. The rest of this paper is organized as follows. In Sec. II, the model is introduced. The results of the wave-kinetic simulation are described, and the obtained zonal staircases are theoretically studied in Sec. III. A summary is presented in Sec. IV.

II. MODEL

In this study, we consider a magnetized plasma with an inhomogeneous density background. The magnetic field and density gradient are chosen to lie along the z and x directions, respectively. The normalizations of space and time are as follows:

$$t \rightarrow c_s L_n^{-1} t, \tag{1}$$

$$x \rightarrow \rho_s^{-1} x, \tag{2}$$

where c_s is the speed of sound, and L_n is the density scale length. As for physical quantities, the density, electrostatic potential, and velocity are normalized as follows:

$$N \rightarrow (L_n \rho_s^{-1}) N, \tag{3}$$

$$\phi \rightarrow (L_n \rho_s^{-1}) e \phi / T_e, \tag{4}$$

$$V \rightarrow (L_n \rho_s^{-1}) V / c_s. \tag{5}$$

In this normalization, the background density gradient is given by $\partial_x N_0 = -1$.

As fundamental processes, we focus on the formation of zonal flows and the associated transport modulations through the interaction of turbulence in phase space. The key processes are summarized in Fig. 1. The evolution equations for the action of turbulence, zonal density, and the zonal flow are given as follows:

$$\partial_t I_k + v_g \partial_x I_k - \partial_x \omega_k \partial_k I_k = \gamma_L I_k - \Delta \omega I_k^2, \tag{6}$$

$$\partial_t \bar{N}' = -\partial_x^2 \Gamma_x + \mu_n \partial_x^2 \bar{N}', \tag{7}$$

$$\partial_t \bar{V}_y = -\partial_x \Pi_{xy} + \nu \partial_x^2 \bar{V}_y. \tag{8}$$

where I_k is the action of turbulence defined as $I_k = (1 + k_\perp^2) |\phi_k|^2$, \bar{N} is the normalized zonal density, and \bar{V}_y is the zonal flow. It is noted

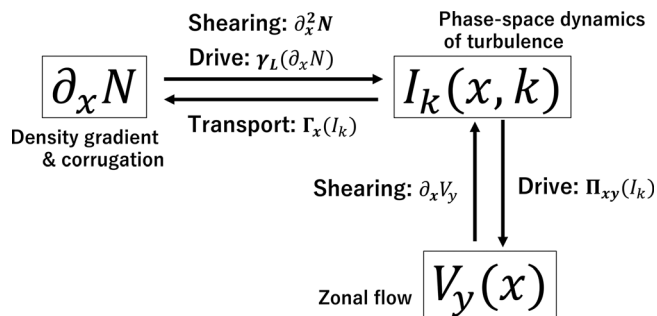


FIG. 1. Schematic view of processes this study focused on: phase space dynamics of turbulence and the formation of zonal flow and density corrugation.

that the action of turbulence I_k does not contain any phase information and reflects the envelope of turbulence. Here, the spatial derivative is denoted by X' , where X is an arbitrary physical quantity. The nonlinear damping of turbulence is denoted by $\Delta \omega$, and the dissipation coefficients for the density and flow are given by μ_n and ν , respectively. The drift wave turbulence is assumed in this study, so that the turbulence dispersion relation ω_k , the group velocity v_g , and the growth rate γ_L are given as follows:

$$\omega_k = \frac{k_y(1 - \bar{N}' + \bar{V}_y'')}{(1 + k_\perp^2)} + k_y V_y, \tag{9}$$

$$v_g = -\frac{2k_x k_y}{(1 + k_\perp^2)^2} (1 - \bar{N}' + \bar{V}_y''), \tag{10}$$

$$\gamma_L = \frac{k_y^2}{C(1 + k_\perp^2)^3} \left\{ k_\perp^2 (1 - 2\bar{N}') - (1 - k_\perp^2) \bar{V}_y'' \right\}. \tag{11}$$

Here, the presented turbulence dispersion properties can be systematically derived from the Hasegawa–Wakatani model near the adiabatic limit. The effects of the zonal density are self-consistently introduced on the modifications of the turbulence dispersion relation. The quasi-linear turbulent fluxes for particles and momentum can be written as follows:

$$\Gamma_x = \int \frac{k_y^2}{C(1 + k_\perp^2)^3} \left\{ k_\perp^2 (1 - \bar{N}') - \bar{V}_y'' \right\} I_k d^2 k, \tag{12}$$

$$\Pi_{xy} = -\int \frac{k_x k_y}{(1 + k_\perp^2)^2} I_k d^2 k. \tag{13}$$

Here, C denotes a parameter that depends on the collisionality; when one considers a resistive drift wave, C is given as $C = Dk_\parallel^2$ (D is the parallel electron diffusion coefficient and k_\parallel is the parallel wavenumber), and when one assumes the trapped electron mode, C is given as $C = \nu_e / \sqrt{\epsilon}$ (ν_e is the electron collision frequency and ϵ is the inverse aspect ratio). The particle flux includes the effect of zonal field, which stems from the modulation of cross-phase between the particle and potential fluctuations, and whose expression can be derived from the Hasegawa–Wakatani model within the framework of the quasi-linear theory.

The presented set of model equations are based on the following assumptions: (1) the wave-kinetic assumption used to derive these model equations requires that the scales of the dynamical variables (the action of turbulence, density, and flow) are much longer than the radial eddy correlation length, which is of order 1 in these normalized equations—thus $q_x \ll 1$ is necessary; (2) the phase difference between the density and potential in turbulence fluctuation is small, $C \gg 1$; and (3) turbulence spreading, which stems from the nonlinear diffusion of turbulence, is ignored. The model includes the higher order spatial derivatives for zonal fields as given in Refs. 21 and 22, and the zonal density effect only for the first order effect. The basis of the treatment of zonal density in the wave-kinetic framework is given in Ref. 23. Here, when one neglects the effects of the zonal field on the dispersion relation and the group velocity, and the second order spatial derivative terms in the growth rate, the model equations agree with those in Ref. 23. When one ignores the zonal density, the model corresponds to that in Refs. 21 and 22. The model in this study is a natural extension of the previous ones.

III. WAVE-KINETIC SIMULATION FOR ZONAL STAIRCASE

A. Simulation settings

The model equations given by Eqs. (6)–(8) are numerically solved with the finite difference method, keeping the dynamics in the phase space (x, k_x) . For the real space x , the periodic boundary condition is used, and Neumann-type boundary conditions are chosen for the wavenumber space, where the derivatives of I_k with respect to k_x are set to zero at the boundary. The simulation is performed with the following parameters: $C = 10$, $k_y = 1$, $\Delta\omega = 0.01$, $\mu_n = 0.05$, $\nu = 0.05$. A spatially homogeneous turbulence spectrum with a small amplitude perturbation for the zonal field is introduced as an initial condition, the time evolutions of I_k , \bar{N} , and \bar{V}_y are calculated.

B. Properties of zonal staircases

In this subsection, the numerical results of the wave-kinetic simulation are shown; the spatiotemporal evolution of turbulence and zonal field is presented. Then, the theoretical basis for the zonal density is discussed.

The time evolution of the turbulence and zonal field energy is illustrated in Fig. 2, where the turbulence and zonal kinetic/thermal energies are, respectively, defined as follows:

$$\mathcal{E} = \int (1 + k_{\perp}^2)^{-1} I_k d^2k, \tag{14}$$

$$E_k = \frac{1}{2} \int \bar{V}_y^2 dx, \tag{15}$$

$$E_N = \frac{1}{2} \int \bar{N}^2 dx. \tag{16}$$

Initially, the action of turbulence is given as $I_k(t=0) = \gamma_L/\Delta\omega$, which is homogeneous in space, as seen in the bottom left panel in Fig. 2. As seen in the top panel of Fig. 2, the zonal flows grow faster than the zonal density, and eventually they saturate with finite amplitudes. The magnitude of zonal density can be seen to be comparable to that of the zonal flow. The bottom panel of Fig. 2 shows snapshots of

the phase space pattern of the action of turbulence. The action of turbulence I_k forms island structures in the phase space when the zonal field has a finite amplitude, which is a consequence of turbulence trapping.^{13–15,24} The excited zonal flow is a low frequency zonal flow; so, it does not show any spatial propagation. Although turbulence have a property to propagate in space with the group velocity presented in Eq. (10), the zonal flow modifies the wavenumber k_x to change the propagation direction and the turbulence is trapped where the zonal flow curvature is negative^{13,25} (for the details, see Appendix). Due to turbulence trapping, the spatial relationships among them holds in the whole period of saturated states.

The time evolution of spatial distributions of the turbulence and zonal fields is shown in Fig. 3. The turbulence intensity, the zonal flow, and zonal density gradient have their maxima at nearly the same position. The peaks of turbulence and zonal field do not propagate. In order to clarify the spatial relationships between zonal flow and density, snapshots of the zonal field and the density profile are illustrated in Fig. 4. As a reference, the phase space pattern of the action of turbulence is shown in the top panel, where the white curve in the contour shows the zonal flow pattern. The zonal flow and zonal density are shown in the middle, and the density profile in which the zonal density is superposed is shown in the bottom. We can see that the phase difference of the zonal density and zonal flow is around $\pi/2$. The gradient of zonal density is positive where the zonal flow has a positive peak, which corresponds to density flattening.

The analytical expression for zonal density is considered in order to understand the spatial relations described above. The zonal density can be evaluated from Eq. (7) by neglecting the time derivative as

$$\bar{N}' \approx \mu_n^{-1} \Gamma_x. \tag{17}$$

Thus, the analytical expression for \bar{N}' is given by

$$\bar{N}' = \frac{1}{\mu_n C} \left[1 + \frac{1}{\mu_n C} \int \frac{k_y^2 k_{\perp}^2}{(1 + k_{\perp}^2)^3} I_k d^2k \right]^{-1} \left[\int \frac{k_y^2 k_{\perp}^2}{(1 + k_{\perp}^2)^3} I_k d^2k - \int \frac{k_y^2}{(1 + k_{\perp}^2)^3} I_k d^2k \bar{V}_y'' \right]. \tag{18}$$

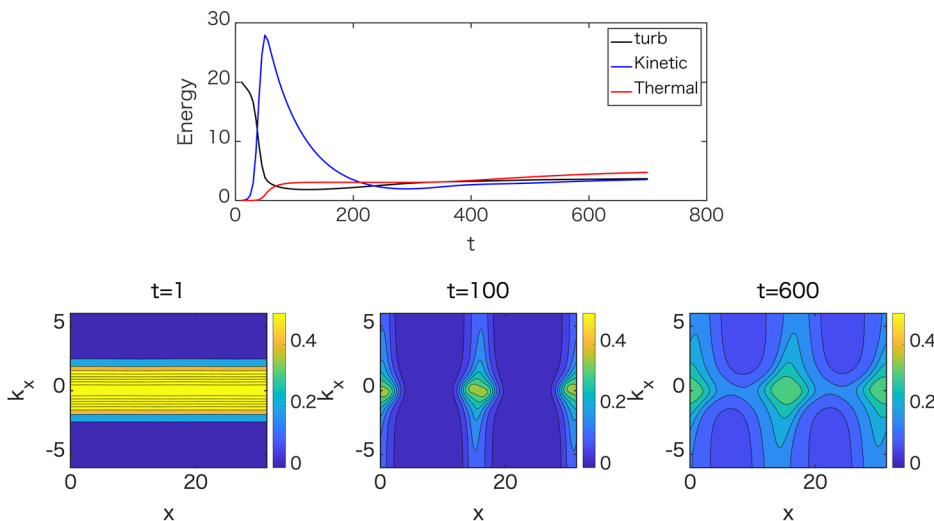


FIG. 2. Upper panel: The time evolution of the energies of turbulence and the zonal fields. The kinetic and thermal energies of zonal fields (E_k , E_N) are calculated from $E_k = 2^{-1} \int \bar{V}_y^2 dx$ and $E_N = 2^{-1} \int \bar{N}^2 dx$, respectively. Bottom panel: Snapshots of the action for turbulent flows I_k in the phase space at $t = 1, 100$, and 600 .

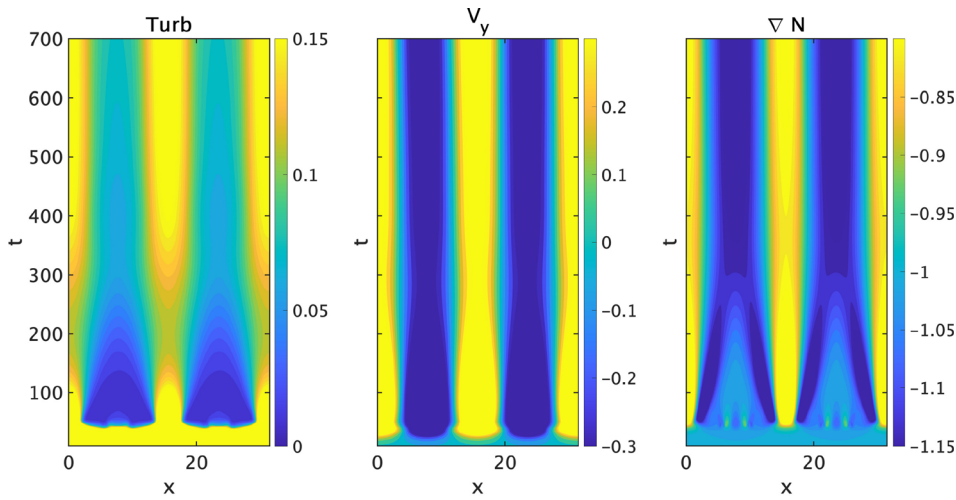


FIG. 3. Spatiotemporal evolutions of turbulence energy (left panel), zonal flow (middle panel), and zonal density gradient (right panel).

Here, the second term in the first bracket (density modulation effect) and the second term in the second bracket (flow curvature effect) stem from the modulation of phase difference between the density and potential in turbulence fluctuation. These terms represent the higher order effect of the zonal field under the assumption of $C \gg 1$ and $q_x \ll 1$. The fundamental effect for the drive of the zonal density is the amplitude modulation of turbulence fluctuation, so the zonal density can be approximated by

$$\bar{N}' \approx \frac{1}{\mu_n C} \int \frac{k_y^2 k_\perp^2}{(1 + k_\perp^2)^3} I_k d^2 k. \quad (19)$$

It is found that the spatial structure of the zonal density gradient agrees with that of turbulence, which captures the characteristics obtained in the simulation shown in Figs. 3 and 4. This can be understood as follows. The turbulence-driven particle flux becomes large in the region where the turbulence is strong, and thus density flattening (the positive density gradient) occurs there, which corresponds to the zonal density. Because of turbulence trapping, the turbulence is accumulated where the curvature of the zonal flow is negative. Therefore, the spatial relationships among zonal field and turbulence can be summarized as follows:

$$\text{sgn}(\bar{N}') \approx \text{sgn}(\bar{V}_y) \approx -\text{sgn}(\bar{V}_y''), \quad (20)$$

$$\text{sgn}(\bar{N}'') \approx \text{sgn}(\bar{V}_y'). \quad (21)$$

These relations hold when the zonal flow has sufficient amplitude for turbulence trapping.

The parameter dependence of the zonal staircase height is discussed. For Eq. (19), the integral in the wavenumber space is evaluated from the turbulence trapping width $\Delta k = \sqrt{2k_y^2 q_x^2 \bar{V}_y / (1 + k_y^2)^2} \sim q_x \sqrt{\bar{V}_y}$, and the turbulence intensity in the trapping region is estimated by $I_{turb} \sim \gamma_L / \Delta \omega$. Then, Eq. (19) can be estimated as follows:

$$\bar{N} \sim \frac{\gamma_L \sqrt{\bar{V}_y}}{8\mu_n C \Delta \omega}, \quad (22)$$

where we assume $k_y \sim 1$. This determines the height of the zonal staircase. Figure 5 shows the comparison of the zonal density obtained from the wave-kinetic simulation and the analytical expression Eq. (22). The numerical result agrees well with Eq. (22). The dimensional form of Eq. (22) for the resistive drift wave turbulence can be expressed by

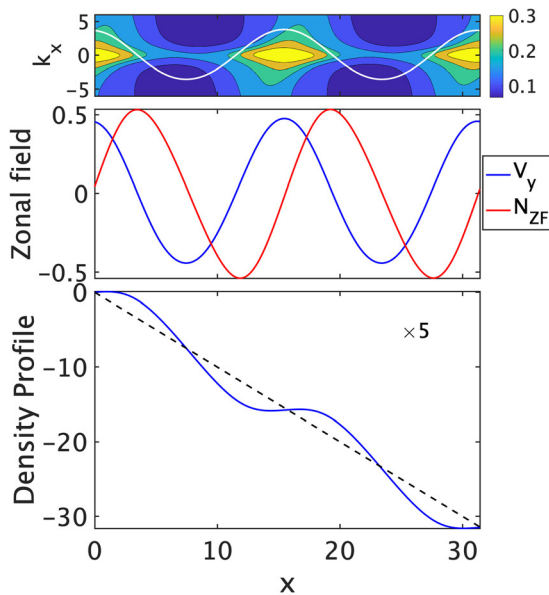


FIG. 4. Spatial relationships between turbulence and zonal density. Upper panel: Snapshot of the action for turbulent flows in the phase space, where the white curve is the zonal flow pattern. Middle panel: Snapshots of zonal field in real space, where blue and red curves correspond to zonal flow and zonal density, respectively. Bottom panel: Snapshot of density profile, which is calculated from the summation of background and zonal density, where the zonal density is displayed by multiplying by five in order to clarify the spatial pattern.

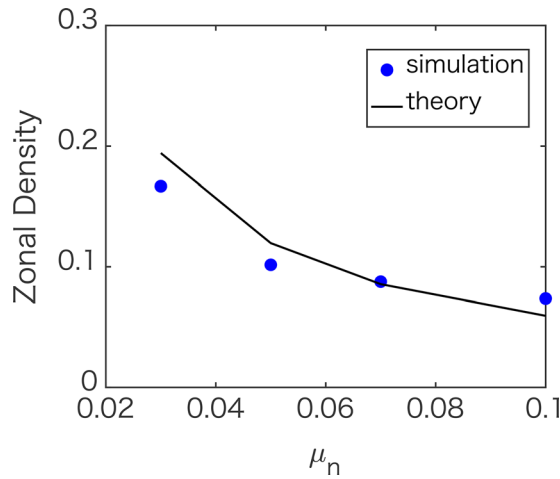


FIG. 5. Dependence of zonal density (zonal staircase) on collisional diffusion coefficient for $C=10$. The zonal density obtained by the simulation is shown in blue dots, and the theoretical expression, Eq. (22), is shown by the back curve.

$$\begin{aligned} \frac{\bar{N}}{N_0} &\sim \frac{1}{8(2\pi)^2} \frac{\nu_e}{\nu_i} \left(\frac{\lambda_{\parallel}}{L_n}\right)^2 \frac{m_i}{m_e} \sqrt{\frac{\bar{V}_y \rho_s}{V_d L_n}}, \\ &\sim \frac{1}{8(2\pi)^2} \left(\frac{qR}{L_n}\right)^2 \left(\frac{m_i}{m_e}\right)^{3/2} \left(\frac{T_i}{T_e}\right)^{3/2} \sqrt{\frac{\bar{V}_y \rho_s}{c_s \rho_s / L_n L_n}}. \end{aligned} \quad (23)$$

Here, the coefficients C and μ_n are evaluated by

$$C = \frac{v_{The}^2 k_{\parallel}^2}{\nu_e c_s / L_n} = (2\pi)^2 \frac{c_s / L_n}{\nu_e} \left(\frac{L_n}{\lambda_{\parallel}}\right)^{3/2} \frac{m_i}{m_e}, \quad (24)$$

$$\mu_n = \frac{\nu_i \rho_s^2}{c_s \rho_s^2 / L_n} = \frac{\nu_i}{c_s / L_n}, \quad (25)$$

where ν_e and ν_i are the electron-ion and ion-ion collisional frequencies, respectively, and their ratio is estimated by $\nu_e / \nu_i \sim \sqrt{m_i / m_e} (T_i / T_e)^{3/2}$. The parallel wavenumber for turbulence is k_{\parallel} , which can be written by the connection length $k_{\parallel} = 2\pi / \lambda_{\parallel}$, where λ_{\parallel} is estimated by qR . It is noted that the presented expression is the zonal staircase height for the resistive drift wave case under the scale separation assumption. A treatment of the more general case is beyond the scope of this study, which should be studied in the future.

It should be noted that the quasi-linear flux evaluated from the mixing length theory, which has been widely used, e.g., Refs. 26 and 27, often cannot predict the spatial profile of turbulent transport correctly especially in the presence of zonal density corrugation. In this approach, turbulence is not treated and only the local gradient length scale is considered, so that the spatially localized turbulence profile cannot be included, and even rather the opposite trend could be obtained. In the presence of the zonal staircase profile, the turbulence and the associated transport are strong where the flow curvature is negative. There, the density gradient is weakened by the zonal density corrugation, and thus the quasi-linear flux becomes small where the real turbulence flux is strong.

C. Roles of staircases on turbulence profile

The roles of the zonal density on the turbulence spatial profile are discussed in this subsection. The spatiotemporal evolution equation of the turbulence energy, $\mathcal{E} = \int (1 + k_{\perp}^2)^{-1} I_k d^2 k$, can be derived by multiplying $(1 + k_{\perp}^2)^{-1}$ in the both sides of Eq. (6) and integrating in the wavenumber-space as follows:

$$\partial_t \mathcal{E} + \partial_x (\widehat{v}_g \mathcal{E}) = W + \widehat{\gamma}_L \mathcal{E} - \widehat{\Delta \omega} \mathcal{E}^2. \quad (26)$$

Each term is defined by

$$\widehat{v}_g \mathcal{E} = \int \frac{\partial_k \omega_k}{1 + k_{\perp}^2} I_k d^2 k = \widehat{v}_{g0} \mathcal{E} \left(1 - \bar{N}' + \bar{V}_y''\right), \quad (27)$$

$$W = 2 \int \frac{k_x \omega_k'}{(1 + k_{\perp}^2)^2} I_k d^2 k = -\widehat{v}_{g0}' \mathcal{E} \left(-\bar{N}'' + \bar{V}_y'''\right) - 2\Pi_{xy} \bar{V}_y', \quad (28)$$

$$\widehat{\gamma}_L \mathcal{E} = \int \frac{\gamma_L}{(1 + k_{\perp}^2)^2} I_k d^2 k = \widehat{\gamma}_{L0} \mathcal{E} - \alpha \mathcal{E} \bar{N}' - \beta \mathcal{E} \bar{V}_y'', \quad (29)$$

$$\widehat{\Delta \omega} \mathcal{E}^2 = \int \frac{\Delta \omega}{(1 + k_{\perp}^2)^2} I_k^2 d^2 k. \quad (30)$$

Here, the coefficients are given as follows:

$$\widehat{v}_{g0} = -\mathcal{E}^{-1} \int \frac{2k_x k_y}{(1 + k_{\perp}^2)^3} I_k d^2 k, \quad (31)$$

$$\widehat{\gamma}_{L0} = \mathcal{E}^{-1} \int \frac{k_y^2 k_{\perp}^2}{C(1 + k_{\perp}^2)^4} I_k d^2 k, \quad (32)$$

$$\alpha = 2\gamma_{L0}, \quad (33)$$

$$\beta = \mathcal{E}^{-1} \int \frac{k_y^2 (1 - k_{\perp}^2)}{C(1 + k_{\perp}^2)^4} I_k d^2 k. \quad (34)$$

The flow shearing effect corresponds to the last term of Eq. (28). Based on the relations shown in Eqs. (20) and (21), one finds that the zonal density and the flow curvature, which are the first and second terms in Eq. (28), have the same effect on turbulence and have opposing effects on flow shearing. Thus, flow shearing is reduced by zonal density and flow curvature. For the turbulence propagation speed, Eq. (27), the zonal density and flow curvature enhance with each other. The modification of turbulence growth due to the zonal density can be found in the second term of Eq. (29), where the zonal density works to suppress the turbulence growth. The mechanism is as follows. The turbulence is trapped where the flow curvature is negative, and as a consequence, the zonal density gradient becomes positive there, as seen in Fig. 4, which can be understood from Eq. (19). It is noted that the zonal flow curvature enhances the effect of zonal density to suppress the turbulence growth.

The roles of zonal density evaluated from the simulation is shown in Fig. 6. The snapshot of the action for turbulent flows in the phase space is shown in the upper panel as a reference. The bottom panel illustrates the profiles of each term in the turbulence energy equation, Eq. (26), where the blue, black, and red curves are the turbulence propagation term (the second term in LHS), shearing term (the first term in RHS), and the growth rate term (the second term in RHS), respectively. The dashed lines correspond to those without the zonal density effect, and the solid lines are the total contributions. The shearing term

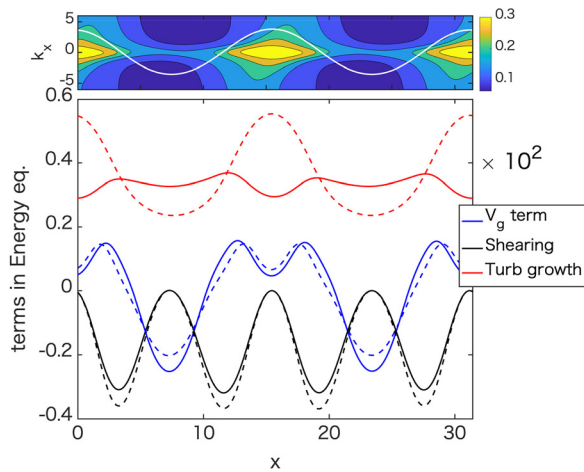


FIG. 6. Roles of each term in turbulence energy equation on turbulence profile. The snapshot of the action of turbulence in the phase space is shown in the upper panel as a reference. The bottom panel illustrates the profiles of each term in turbulence energy equation, Eq. (26), where the blue, black, and red curves are the turbulence propagation term, shearing term, and the growth rate term, respectively. The dashed lines correspond to those without the zonal density effect, and the solid lines are the total contributions.

is negative in the whole region (turbulence suppression), but the propagation term changes its sign, which is the same order of magnitude with the shearing term. For these terms, the zonal density effect is not the dominant effect. For the growth rate, the zonal density effect is important. Due to the effect of zonal density, the turbulence growth becomes flattened, which competes with the localization of turbulence due to trapping. Thus, the turbulence profile is determined by the competition between turbulence trapping and profile flattening caused by the effect of zonal density. In the presented situation, it is found that turbulence trapping dominates profile flattening due to the effect of zonal density.

Finally, we discuss the phase space patterns of the turbulent fluxes for the momentum and the particle for future validation in simulations or experiments, which is shown in Fig. 7. The magnitude of momentum flux is strong, where the turbulence is accumulated (the negative region for the flow curvature). Because the positive/negative sign of the momentum flux depends on the sign of k_x , and thus, the momentum flux in the real space, which is integrated in k_x , captures the asymmetry part so that the momentum flux is strong in the region where the flow shear is strong. The particle flux, which is independent of the sign of k_x , is strong where the turbulence is strong, for the phase space as well as in the real space. The dashed lines correspond to those without the zonal density effect, and the solid lines represent the total contributions. It can be seen that the zonal density plays a role in the flattening of the growth rate. These structures determine the characteristics of the zonal staircases. It should be noted that the particle flux presented in this paper is evaluated quasi-linearly. In other words, while the zonal flow effect on the turbulence intensity is taken into account based on the wave-kinetics, the effect of zonal flow on the phase modulation between the potential and the density in the turbulent component is not perfectly considered. An extension of this study that includes the phase dynamics should be investigated in the future.

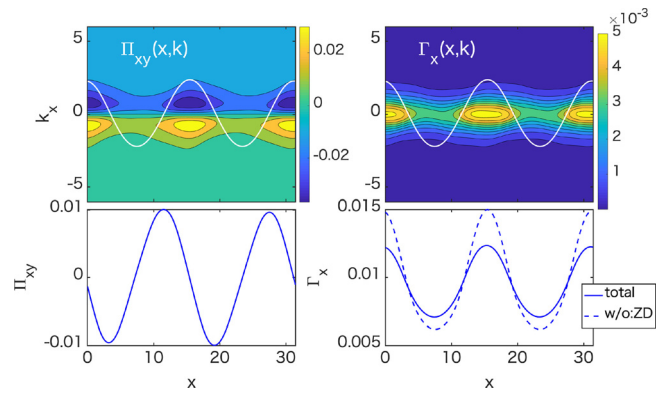


FIG. 7. Spatial pattern of the turbulent fluxes: Left panel shows the profile of the momentum flux in the phase space (upper), and in the real space (bottom), where the real space pattern is obtained from the integral of the wavenumber space. Right panel shows the particle flux in the phase space (upper), and in the real space (bottom). For the real space pattern, the cases with and w/o the zonal density are shown in solid and dashed lines, respectively. The dashed lines correspond to those without the zonal density effect, and the solid lines are the total contributions.

IV. SUMMARY

Density corrugation due to zonal flow, so-called zonal staircase, is investigated, based on wave-kinetic simulation. The simulation is developed by considering profile corrugations and the turbulence trapping mechanism. The modification of profiles and the dispersion relation in turbulence are included, based on the assumption of scale separation for turbulence and zonal field and the phase relationship for the turbulence fluctuations. We obtain the analytical expression for the zonal density (the staircase height), which is driven by the modulation of particle transport. It is found that the normalized zonal density can be comparable to the zonal flow normalized by the diamagnetic drift velocity. However, under the circumstances in this study, the density corrugations that stems from the zonal density are too small to strongly modify the turbulence intensity pattern. This is because the diffusive flux dominates; so the density fluctuations are relatively unimportant. The key effect that determines the turbulence profile is found to be turbulence trapping by the zonal flow, while the profile corrugation due to the effect of zonal density has weaker effects. Thus, turbulence is localized where the flow curvature is negative, which leads to a flattening of the density profile through the enhancement of particle transport. This fact clearly shows that the effect of turbulence trapping dominates the density gradient dependence of the local linear instability.

ACKNOWLEDGMENTS

The authors acknowledge the stimulating discussions they had with and strong support provided by Professor S. -I. Itoh. This paper is dedicated to her memory. This work was partly supported by JSPS Kakenhi Grant Nos. JP21K03509, JP21K03513, JP17H06089, JP16H02442, and JP15H02155, the collaboration programs of NIFS (No. NIFS21KNST194), Kyushu University RIAM (2021 S3-2), and the Nihon University Fund for Supporting Young Scientists.

AUTHOR DECLARATIONS

Conflict of Interest

The authors have no conflicts to disclose.

DATA AVAILABILITY

The data that support the findings of this study are available from the corresponding author upon reasonable request.

APPENDIX: TURBULENCE TRAPPING IN ZONAL FLOW

Turbulence trapping can be understood from the turbulence trajectory in phase space, which is the characteristic curve of Eq. (6) in the case where the growth and nonlinear damping of turbulence are absent. In order to clarify the flow effect on the turbulence dynamics, here, we neglect the effects of the zonal density and the higher order spatial derivatives, and only the fundamental terms are considered. The turbulence trajectory in phase space $(x(t), k_x(t))$ is governed by^{13,25}

$$\frac{dx(t)}{dt} = -\frac{2k_x(t)k_y}{(1+k_x(t)^2+k_y^2)^2}, \quad (\text{A1})$$

$$\frac{dk_x(t)}{dt} = -k_y V_y(x(t))'. \quad (\text{A2})$$

From this set of equations, we obtain

$$\frac{d^2x(t)}{dt^2} \approx \left[\frac{2k_y^2 V_y''}{(1+k_0^2+k_y^2)^2} \right] x(t), \quad (\text{A3})$$

where k_0 is the time average value of $k_x(t)$. From this, we found that when $V_y'' < 0$, the solution of $x(t)$ is the oscillation, which is the turbulence trapping, and when $V_y'' > 0$, the turbulence exponentially propagates, which is the exclusion of the turbulence. In this way, the asymmetry with respect to the sign of the flow curvature on the turbulence dynamics appears.

REFERENCES

- ¹M. C. Gregg and T. B. Sanford, "Shear and turbulence in thermohaline staircases," *Deep Sea Res., Part A* **34**(10), 1689–1696 (1987).
- ²P. S. Marcus, "Jupiter's great red spot and other vortices," *Annu. Rev. Astron. Astrophys.* **31**(1), 523–569 (1993).
- ³G. Dif-Pradalier, P. H. Diamond, V. Grandgirard, Y. Sarazin, J. Abiteboul, X. Garbet, P. Ghendrih, A. Strugarek, S. Ku, and C. S. Chang, "On the validity of the local diffusive paradigm in turbulent plasma transport," *Phys. Rev. E* **82**(2), 025401 (2010).
- ⁴A. Ashourvan and P. H. Diamond, "On the emergence of macroscopic transport barriers from staircase structures," *Phys. Plasmas* **24**(1), 012305 (2017).
- ⁵G. Dif-Pradalier, G. Hornung, P. Ghendrih, Y. Sarazin, F. Clairet, L. Vermare, P. H. Diamond, J. Abiteboul, T. Cartier-Michaud, C. Ehrlacher *et al.*, "Finding the elusive $E \times B$ staircase in magnetized plasmas," *Phys. Rev. Lett.* **114**(8), 085004 (2015).
- ⁶W. Wang, Y. Kishimoto, K. Imadera, J. Q. Li, and Z. X. Wang, "A mechanism for the formation and sustainment of the self-organized global profile and $E \times B$ staircase in tokamak plasmas," *Nucl. Fusion* **58**(5), 056005 (2018).
- ⁷L. Qi, J.-M. Kwon, T. S. Hahm, S. Yi, and M. J. Choi, "Characteristics of trapped electron transport, zonal flow staircase, turbulence fluctuation spectra in elongated tokamak plasmas," *Nucl. Fusion* **59**(2), 026013 (2019).
- ⁸L. Qi, M. J. Choi, J.-M. Kwon, and T.-S. Hahm, "Role of zonal flow staircase in electron heat avalanches in kstar l-mode plasmas," *Nucl. Fusion* **61**(2), 026010 (2020).
- ⁹H. Arakawa, T. Kobayashi, S. Inagaki, N. Kasuya, S. Oldenbürger, Y. Nagashima, T. Yamada, M. Yagi, A. Fujisawa, K. Itoh *et al.*, "Dynamic interaction between a solitary drift wave structure and zonal flows in a linear cylindrical device," *Plasma Phys. Controlled Fusion* **53**(11), 115009 (2011).
- ¹⁰W. Liu, Y. Chen, R. Ke, G. McKee, Z. Yan, K. Fang, Z. Yang, Z. Gao, Y. Tan, and G. R. Tynan, "Evidence of $E \times B$ staircase in HL-2A L-mode tokamak discharges," *Phys. Plasmas* **28**(1), 012512 (2021).
- ¹¹A. Ashourvan, R. Nazikian, E. Belli, J. Candy, D. Eldon, B. A. Grierson, W. Guttenfelder, S. R. Haskey, C. Lasnier, G. R. McKee *et al.*, "Formation of a high pressure staircase pedestal with suppressed edge localized modes in the diii-d tokamak," *Phys. Rev. Lett.* **123**(11), 115001 (2019).
- ¹²M. J. Choi, H. Jhang, J.-M. Kwon, J. Chung, M. Woo, L. Qi, S. Ko, T.-S. Hahm, H. K. Park, H.-S. Kim *et al.*, "Experimental observation of the non-diffusive avalanche-like electron heat transport events and their dynamical interaction with the shear flow structure," *Nucl. Fusion* **59**(8), 086027 (2019).
- ¹³M. Sasaki, K. Itoh, K. Hallatschek, N. Kasuya, M. Lesur, Y. Kosuga, and S.-I. Itoh, "Enhancement and suppression of turbulence by energetic-particle-driven geodesic acoustic modes," *Sci. Rep.* **7**(1), 1–7 (2017).
- ¹⁴M. Sasaki, T. Kobayashi, K. Itoh, N. Kasuya, Y. Kosuga, A. Fujisawa, and S.-I. Itoh, "Spatio-temporal dynamics of turbulence trapped in geodesic acoustic modes," *Phys. Plasmas* **25**(1), 012316 (2018).
- ¹⁵X. Garbet, O. Panico, R. Varennes, C. Gillot, G. Dif-Pradalier, Y. Sarazin, E. Bourne, V. Grandgirard, P. Ghendrih, D. Zarzoso *et al.*, "Zonal instability and wave trapping," *J. Phys.: Conf. Ser.* **1785**, 012002 (2021).
- ¹⁶C. Gillot, G. Dif-Pradalier, X. Garbet, O. Panico, Y. Sarazin, R. Varennes, and D. Zarzoso, "Investigation of tokamak turbulent avalanches using wave-kinetic formulation in toroidal geometry," *J. Plasma Phys.* **87**, 905870221 (2021).
- ¹⁷B. F. McMillan, P. Hill, A. Bottino, S. Jolliet, T. Vernay, and L. Villard, "Interaction of large scale flow structures with gyrokinetic turbulence," *Phys. Plasmas* **18**(11), 112503 (2011).
- ¹⁸P. H. Diamond and T. S. Hahm, "On the dynamics of turbulent transport near marginal stability," *Phys. Plasmas* **2**(10), 3640–3649 (1995).
- ¹⁹Y. Kosuga, P. H. Diamond, and Ö. D. Gürçan, "How the propagation of heat-flux modulations triggers $E \times B$ flow pattern formation," *Phys. Rev. Lett.* **110**(10), 105002 (2013).
- ²⁰A. Ashourvan and P. H. Diamond, "How mesoscopic staircases condense to macroscopic barriers in confined plasma turbulence," *Phys. Rev. E* **94**(5), 051202 (2016).
- ²¹J. B. Parker, "Numerical simulation of the geometrical-optics reduction of CE2 and comparisons to quasilinear dynamics," *Phys. Plasmas* **25**(5), 055708 (2018).
- ²²J. B. Parker, "Dynamics of zonal flows: Failure of wave-kinetic theory, and new geometrical optics approximations," *J. Plasma Phys.* **82**(6), 1–13 (2016).
- ²³M. Leconte and T. Kobayashi, "Zonal profile corrugations and staircase formation: Role of the transport crossphase," *Phys. Plasmas* **28**(1), 014503 (2021).
- ²⁴P. H. Diamond, S. I. Itoh, K. Itoh, and T. S. Hahm, "Zonal flows in plasma—a review," *Plasma Phys. Controlled Fusion* **47**(5), R35 (2005).
- ²⁵P. Kaw, R. Singh, and P. H. Diamond, "Coherent nonlinear structures of drift wave turbulence modulated by zonal flows," *Plasma Phys. Controlled Fusion* **44**(1), 51 (2001).
- ²⁶M. J. Pueschel, P.-Y. Li, and P. W. Terry, "Predicting the critical gradient of itg turbulence in fusion plasmas," *Nucl. Fusion* **61**(5), 054003 (2021).
- ²⁷G. M. Staebler, J. E. Kinsey, and R. E. Waltz, "A theory-based transport model with comprehensive physics," *Phys. Plasmas* **14**(5), 055909 (2007).